EUROPEAN ORGANIZATION FOR NUCLEAR RESEARCH

CERN-EP/80-120
4 July 1980

MEASUREMENT OF DIFFRACTIVE 3π PRODUCTION ON A POLARIZED TARGET AT 17 GeV/c

V. Chabaud, J. de Groot, B. Hyams, T. Papadopoulou*) and P. Weilhammer

CERN, Geneva, Switzerland.

B. Niczyporuk, K. Rybicki and M. Turała

Institute of Nuclear Physics, Cracow, Poland.

H. Becker**), G. Blanar, W. Blum, M. Cerrada***), H. Dietl, J. Gallivan,

B. Gottschalk†), E. Lorenz, G. Lütjens, G. Lutz, W. Männer,

D. Notz††), R. Richter, U. Stierlin, B. Stringfellow†††) and F. Wagner

Max-Planck Institute, Munich, Germany.

(Submitted to Nuclear Physics B)

---

*) Now at the National Technical University, Athens, Greece.

**) Now at Technische Fachhochschule, Saarbrücken, Germany.

***) Now at CERN, Geneva, Switzerland.

†) Visitor from Northeastern University, Boston, Mass., USA.

††) Now at DESY, Hamburg, Germany.

†††) Now at the Nuclear Research Centre, Strasbourg, France.

ABSTRACT

The reaction $\pi^- p_\uparrow \to \pi^-\pi^+\pi^- p$ has been measured at 17 GeV/c using a polarized target. The data sample contains about 60,000 interactions on polarized protons. The nucleon polarization as a function of momentum transfer is very similar to elastic $\pi^- p$ scattering and is nearly independent of the 3π mass, except for a possible structure around 1.2 GeV.

Using the isobar model, we have performed a partial wave analysis and extracted the 3π amplitudes. The generalized 3π density matrix elements agree with earlier determinations. Relative phases obtained from density matrix elements agree well with the ones obtained from transversity amplitudes. This proves the validity of the coherence assumption made in the interpretation of unpolarized target results. Our results confirm the existence of an A_1 resonance in the region 1.2-1.3 GeV.

1. INTRODUCTION

In order to understand the mechanism of polarization in diffractive processes, a measurement of the polarization in the reaction

$$\pi^- p_\uparrow \to \pi^-\pi^+\pi^- p \qquad (1)$$

is important. A universal mechanism and/or the Deck model predict(s) the nucleon polarization in reaction (1) to be similar to that observed in the elastic $\pi^- p$ reaction. Semi-inclusive duality [1] predicts a linear increase of polarization with 3π mass.

Another interesting subject is the presence of resonances in the 3π system, especially the A_1. The experimental evidence for such a state has been controversial over the last 10 years. Backward production of $\rho\pi$ [2] seemed to indicate a 200 MeV wide resonance around 1.05 GeV. The structure observed in the heavy lepton decay $\tau \to (3\pi)\nu$ [3] might also indicate the presence of the A_1. On the other hand, results from charge and hypercharge exchange reactions [4] have provided only upper limits for the A_1 production cross-section. The lack of sufficient statistics to perform a detailed partial wave analysis has been a general feature of the above-mentioned experiments.

Most of the A_1 searches have been made on the quasi-elastic reaction $\pi^\pm \to \pi^\pm\pi^+\pi^- p$ [5,6]. In all experiments a large enhancement around 1.1 GeV is observed in the 3π mass spectrum. Although the $J^P = 1^+$ state is the dominant one in the low-mass region, a simple resonance behaviour cannot explain the data, especially not the t-dependent shape of the $J^P = 1^+$ intensity. A solution was proposed by several groups [7,8]. In these models, resonance production proceeds by two mechanisms, one being the usual resonance production (direct term) and the other a background (possibly given by the Deck mechanism) modified by rescattering. As shown in the recent analysis of high statistics data by the Amsterdam-CERN-Cracow-Munich-Oxford-Rutherford (ACCMOR) Collaboration [5], both contributions are present and led to the observed 1^+ spectra requiring an A_1 resonance with a mass of 1.28 GeV and a width of 300 MeV.

In unpolarized target experiments, when using relative phases from density matrix elements, there is the additional assumption that relative phases between nucleon spin-flip and spin-non-flip amplitudes are the same (coherence assumption). In this paper we present the results obtained in the analysis of reaction (1) at 17 GeV/c using a polarized target. Such an experiment allows an amplitude analysis to be performed, and the relative phases between amplitudes can be measured. Even if we cannot compete with ref. [5], as far as acceptance and statistics are concerned, we can make a test of the coherence assumption.

The paper is organized in the following way. In section 2 we describe the experimental set-up and some relevant features of the data. Section 3 contains a description of the formalism and method used in this analysis. Details on the partial wave analysis and some checks on the method are given in section 4. In section 5 we discuss the results, and section 6 contains our conclusions.

2. EXPERIMENTAL DETAILS

2.1 Experimental set-up

The experiment was performed with the CERN-Munich spectrometer at the CERN Proton Synchrotron (PS); this spectrometer has been described in detail elsewhere [9]. A schematic top view of the experimental set-up is shown in fig. 1. The incident pions are identified by the threshold Čerenkov counter $\check{C}_1$ and momentum analysed with the beam spectrometer. The beam is defined by the coincidence of signals of the scintillation counters B_1, B_2, and B_3, and the anticoincidence of B_4, a counter with an 18 mm circular hole in it. A butanol target (100 mm long, 20 mm in diameter) in a 2.5 T field was used. It was transversely polarized (average polarization 68%), and the sign of the polarization was inverted daily in order to have roughly the same amount of data with each sign (up and down). A fraction of the data was taken using a hydrogen target of identical shape for calibration purposes. A hodoscope of 36 1 mm thick scintillation counters A_i around the target defined 72 equal bins in the recoil azimuth. It was not included in the trigger, but its information was recorded in pattern units. Six wider, 1 mm thick counters F_1-F_6 were used to demand one recoil and, behind each of these, six scintillator/tungsten sandwich counters F_7-F_{12} vetoed γ-rays from low-energy π^0's.

The forward-produced charged secondaries were momentum analysed with spark chambers (SCh) before and after the AEG spectrometer magnet (150 × 50 cm gap window and 2 T·m bending power). Multiwire proportional chambers (MWPC) just in front of and behind the target were used to improve vertex determination. Secondary pions were identified in the Čerenkov counter $\check{C}_2$ (pion threshold 4.7 GeV). The Čerenkov counter $\check{C}_3$ was not used for this experiment (it allowed discrimination between kaons and protons above 8.5 GeV). A multiplicity of three was demanded in the 32-element hodoscope EG, which consisted of 100 mm wide vertical counters.

2.2 Data distribution

A total of 1.6 million triggers were recorded on tape and processed by a geometrical reconstruction program, and only events with three secondary tracks coming from a vertex inside the target were accepted. Since we have a butanol target, a significant fraction of the interactions are on bound (unpolarized) protons. In order to enhance the fraction of events on free (polarized) protons, we exploited the target hodoscope described in section 2.1. We studied the difference between the azimuthal angle of the recoil proton, as measured by this hodoscope, and that of the reaction plane defined by the incoming beam and the forward 3π system. This difference $\Delta\Phi$ is a measurement of the coplanarity of the event, and its distribution is shown in fig. 2. The large peak at 0° corresponds to events produced on free protons. From the study of this distribution, we can estimate the amount of background from interactions on bound protons which is present in our data sample (see Appendix 1). After applying a cut of $|\Delta\Phi| < 5^\circ$, it is of the order of 25%. We assume that the only effect of these background events is to reduce the degree of polarization, and this was checked by comparing butanol target and hydrogen target data samples. No significant difference was found in $m_{3\pi}$, t, $m_{\pi\pi}$, and (3π) angular distributions. We have also observed no difference between the hydrogen and butanol target data samples in $\pi^+\pi^-$ production with a polarized target [10].

The missing-mass squared (MM^2) distribution is shown in fig. 3. We select events with $MM^2 < 1.35$ GeV^2. From the shape below and above the proton mass, we conclude that the background of events with recoiling N^*'s is smaller than 2%. We reduce the background from the reactions

$$\begin{aligned} \pi^- p_\uparrow &\to K^+K^-\pi^- p \\ \pi^- p_\uparrow &\to p\bar{p}\pi^- p \end{aligned} \qquad (2)$$

by using the Čerenkov information. After applying selection criteria, the contamination from reactions (2) is estimated to be < 2%.

In fig. 4a we show the $|t|$ distribution. In our trigger a signal in the F counters around the target is required. This explains the loss of events in the low $|t|$ region, since low-energy protons do not reach the counters. The accumulation of events in the very low $|t|$ bin is mostly accounted for by the very steep coherent production on nuclei, together with a δ-ray satisfying the trigger condition. Therefore in our analysis we will consider only events with $|t| > 0.1$ GeV^2. The final sample after all cuts contains 60,000 interactions on polarized protons.

In fig. 4b we present the uncorrected 3π mass distribution for the $|t|$ interval $0.1 < |t| < 1.0$ GeV^2; this exhibits a broad enhancement around 1.1 GeV and a signal in the A_2 region. The A_2 shows up more clearly at high $|t|$ values. The $\pi^+\pi^-$ and $\pi^-\pi^-$ mass distributions are also presented in figs. 5a and 5b. The former shows strong ρ production.

Since we collected data with target polarization up and down, polarization effects can be simply looked for by measuring the left-right asymmetry. One considers the distribution

$$A(\phi) = \frac{N_{up}(\phi) - N_{down}(\phi)}{N_{up}(\phi) + N_{down}(\phi)} , \qquad (3)$$

where $N_{up}(\phi)$ $[N_{down}(\phi)]$ is the observed azimuthal distribution of the 3π system for events with polarization up (down). If the acceptance were the same for all 3π partial waves, the nucleon polarization P_N could be obtained directly from

$$A(\phi) = P_N \times f \times \sin\phi , \qquad (4)$$

f being the effective target polarization (average polarization × fraction of interactions on free protons); $A(\phi)$ is presented in fig. 6 for the full data sample used in the partial wave analysis, and it shows the existence of definite polarization effects in reaction (1). The superimposed curve is a fit to the expression $A(\phi) = \alpha \times \sin \phi$, giving $\alpha = 0.052 \pm 0.003$.

The geometrical acceptance of the spectrometer is 35% for phase-space events at $m_{3\pi} = 1.1$ GeV, and it decreases for higher masses ($\sim$ 15% at $m_{3\pi} = 1.4$ GeV). This prevents us making a partial wave analysis of the high-mass region. In the present work we restrict ourselves to $m_{3\pi} < 1.4$ GeV.

3. METHOD OF ANALYSIS

For a given beam momentum, eight variables are needed to describe reaction (1). We choose them to be $\tau \equiv \{m_{3\pi}, t, \alpha, \beta, \gamma, w, \theta, \psi\}$; $m_{3\pi}$ and t are the 3π invariant mass and the four-momentum transfer between the initial and final protons. If we label the three pions a, b, c (their momenta in the 3π rest frame being q_a, q_b, q_c) for a given dimeson system bc (isobar), then α_a, β_a, γ_a are the three Euler angles describing the transformation from the Gottfried-Jackson frame to the system described by a z-axis in the q_a direction and a y-axis normal to the 3π plane ($\vec{q}_b \times \vec{q}_c$); w_a and θ_a are the invariant mass of the isobar and the angle of the b pion momentum in the isobar rest frame with respect to the q_a direction. The baryon angle ψ containing the polarization information is defined in the over-all centre-of-mass system, the z-axis being the incoming proton direction and the y-axis the normal to the production plane. This choice has the advantage that the target polarization vector $\vec{P}_T$ in the laboratory lies in the x-y plane, with the x and y components being given by $|\vec{P}_T| \sin \psi$ and $|\vec{P}_T| \cos \psi$, respectively.

The differential cross-section for reaction (1) can be expanded in the form [11]:

$$\frac{d\sigma}{d\tau} = \sum_{\substack{K,\eta,S \\ \bar{K},\bar{\eta},\bar{S}}} \tilde{D}_{K\eta}\left(\alpha_a,\beta_a,\gamma_a\right) \times T_S^{K\eta}\left(m_{3\pi},t,w_a\right) \times B_{\eta\bar{\eta}}^{S\bar{S}}(\psi) \times \left(\tilde{D}_{\bar{K}\bar{\eta}} \times T_{\bar{S}}^{\bar{K}\bar{\eta}}\right)^* , \qquad (5)$$

where K stands for $\{J^P Mj\ell\}$, J^P being the spin and parity of the 3π system, M the absolute value of the third component in the Gottfried-Jackson frame, j the spin of isobar, and ℓ its orbital angular momentum with respect to the third pion. The values $\eta = \pm 1$ are related to the naturality of the exchange [12], and $S = \pm 1/2$ labels the transversity amplitudes in the S-channel helicity frame of the baryons. These mixed amplitudes T are the quantities we determine from the data. $\tilde{D}$ and B are known functions containing the information of the 3π decay variables and ψ, respectively. The explicit form of $\tilde{D}$ can be found in ref. [11]. The B matrix is given in Appendix 2.

In order to visualize which target proton and recoil proton spin states correspond to the T amplitudes, we use the symbols ($\uparrow$) and ($\downarrow$) for nucleon polarization upwards and downwards with respect to the reaction plane:

	P_{target}	P_{recoil}
$T^{K1}_{1/2}$	$\uparrow$	$\uparrow$
$T^{K1}_{-1/2}$	$\downarrow$	$\downarrow$
$T^{K-1}_{1/2}$	$\downarrow$	$\uparrow$
$T^{K-1}_{-1/2}$	$\uparrow$	$\downarrow$

Present-day statistics are not sufficient for determining the T amplitudes as a function of the three variables. Therefore we must use the so-called isobar model [13], which makes the following two assumptions:

i) The dependence on w_a can be factorized out of T in the following way:

$$T_S^{K\eta}(m_{3\pi},t,w_a) = T_S^{K\eta}(m_{3\pi},t) \times BW^{j\ell}(w_a) \ , \qquad (6)$$

where BW contains the best knowledge we have of $\pi\pi$ interactions. We have used Breit-Wigner parametrizations for the P- and D-waves, and $\pi\pi$ phase shifts information for the S-wave [14]. From now on we will include BW in the D functions:

$$\tilde{D} \times BW = D \ . \qquad (7)$$

ii) Partial waves with high values of j and ℓ are included by averaging, in the D function, the two possible $\pi^+\pi^-$ combinations forming the isobar, each having in the expansion only low values of J, ℓ, j. Then expression (5) becomes

$$\frac{d\sigma}{dt} = \sum_{\substack{K,\eta,S \\ \bar{K},\bar{\eta},\bar{S}}} D_{K\eta}(\alpha,\beta,\gamma,\theta,w_a) \times T_S^{K\eta}(m_{3\pi},t) \times B_{\eta\bar{\eta}}^{S\bar{S}}(\psi) \times \left(D_{\bar{K}\bar{\eta}} \times T_{\bar{S}}^{\bar{K}\bar{\eta}}\right)^* , \qquad (8)$$

where K is now restricted to low values of J, j, and ℓ.

For a given $(m_{3\pi},t)$ bin, the T amplitudes can be determined up to two arbitary phases. From the amplitudes, we can obtain the 3π density matrix

$$\rho_{K\bar{K}}^{\eta} = \sum_S T_S^{K\eta} \times \left(T_S^{\bar{K}\eta}\right)^* \qquad (9)$$

and the partial cross-sections

$$\sigma_{K\eta} = \sum_S T_S^{K\eta}\left(T_S^{K\eta}\right)^* N_{K\eta} , \qquad (10)$$

where $N_{K\eta}$ denotes the integral over the phase space τ,

$$N_{K\eta} = \int D_{K\eta}\, D_{K\eta}^*\, d\tau . \qquad (11)$$

Partial nucleon polarization can be expressed as

$$P_{K\eta} = \left(T_{-1/2}^{K\eta}\left(T_{-1/2}^{K\eta}\right)^* - T_{1/2}^{K\eta}\left(T_{1/2}^{K\eta}\right)^*\right) \times N_{K\eta}/\sigma_{K\eta} . \qquad (12)$$

The unknown amplitudes T in eq. (8) are determined from the data by using an extended maximum likelihood method [15]. The likelihood function is given by

$$\log \mathcal{L} = \sum_{i=1}^{N_{events}} w_i \log \frac{d\sigma}{d\tau}(\tau_i,T) - \int d\tau\, \mathrm{Acc}\,(\tau)\, \frac{d\sigma}{d\tau}(\tau,T) , \qquad (13)$$

where w_i are weights taking into account losses due to decays in flight or secondary interactions in the target, and Acc describes the acceptance (= 1 for events accepted by the spectrometer and trigger requirements, 0 otherwise). The necessary integrals in eq. (13) as well as the normalization integrals (11) have been calculated using Monte Carlo generated events. Typically we generated 20 Monte Carlo events per real event.

The statistical errors can be computed by the error matrix,

$$E_{K\eta S,\bar{K}\bar{\eta}\bar{S}} = \left[\frac{\partial^2 \log}{\partial T_S^{K\eta} \times \partial T_{\bar{S}}^{\bar{K}\bar{\eta}}} \right]^{-1} . \qquad (14)$$

Since systematic errors are not included, values calculated from eq. (14) will underestimate the true errors. The errors we give in section 5 should be considered approximate.

We close this section by pointing out some important differences between our amplitude analysis and the Ascoli method [16]:

i) In the latter, the free parameters are the density matrix elements; and in practical applications the additional assumption of factorization is made in the following way:

$$\rho^{\eta}_{K\bar{K}} = \rho^{\eta}_{JM,\bar{J}\bar{M}} \times C_K \times C^{*}_{\bar{K}} , \qquad (15)$$

where C is a complex decay amplitude.

ii) In general, the rank of the density matrix ρ^{η} cannot be larger than 2. This restriction is ignored in the Ascoli approach.

Consequently both methods can lead to somewhat different answers for ρ^{η}, even when the same data are used. Another consequence of the extra assumptions is that the fit is linear in $\rho^{\eta}_{JM,\bar{J}\bar{M}}$, which means that the solution is essentially unique, whereas the amplitude analysis could have several solutions.

4. DESCRIPTION OF THE PARTIAL WAVE ANALYSIS AND CONSISTENCY CHECKS

The partial waves used in our analysis are listed in Table 1; this basic set is essentially the same as the one used in previous analyses. Partial waves with $\eta = -1$ were tried and their contribution was found to be negligible. In a first step we used 100 MeV wide $m_{3\pi}$ bins and three t-bins to determine the rough t-dependence in each partial wave. Each partial wave cross-section was fitted by the expression $|t|^M \times e^{at}$.

In a second step we used one large t-bin ($0.1 < |t| < 0.3$ GeV) and 25 MeV $m_{3\pi}$ bins, and the t-dependence previously obtained was incorporated in the

parametrization of independent partial wave amplitudes. The choice of the t-bin was motivated partly by statistical requirements (at least 2000 events/bin) and partly to have maximum sensitivity to the polarization (see below).

At each mass bin, we fitted the data starting from random values of the T amplitudes ($\sim$ 20 searches). Between one and five different solutions were obtained at each energy. The ambiguities affected mainly the minor partial waves, the total intensities being unique but not individual amplitudes. In the following we discuss features of our solutions which do not depend on the ambiguities.

Monte Carlo events weighted with the amplitudes obtained from the fits were generated, passed through the apparatus, and compared with data to check the quality of the fit. A good agreement was obtained.

A measurement of the reaction

$$\pi^- p_\uparrow \to K^- K^0 p \tag{16}$$

in the same experiment [17] provided a good opportunity to test the method of analysis. In this reaction a very clean A_2 is produced with less than 10% background, and its two-body decay is free of isobar model assumptions. Thus we can compare the A_2 results in both decay models. In the region $1.2 < m_{KK} < 1.4$ GeV and $|t| > 0.1$ GeV, 1000 events are available in the $K\bar{K}$ mode.

Using the notation of three-meson states $K \equiv \{J^P M \ell j\}$, the situation can be considered as a simple case where

i) there is only one possible combination to form the dimeson system, namely the K^0;

ii) $j = 0$ since the spin of K^0 is 0. This implies $J = \ell$. Furthermore, no dimeson mass dependence is needed. Basically the $\tilde{D}_{K\eta}$ function of section 3 can be written as

$$\tilde{D}_{K\eta} \equiv \left[Y^J_M(\alpha,\beta) + \eta\, Y^J_{-M}(\alpha,\beta) \right], \tag{17}$$

Y^J_M being the spherical harmonics. By inserting $\tilde{D}_{K\eta}$ in expression (8) instead of $D_{K\eta}$, we can use the same analysis formalism and programs.

We consider as possible states $J^P = 2^+$ ($M = 0$, $\eta = -1$, and $M = 1$, $\eta = \pm 1$) to describe the A_2 and $J^P = 0^-$ ($\eta = +1$) to describe the background. Our results show that the 2^+ contribution is entirely $M = 1$, $\eta = +1$ (other 2^+ states are less than 5%, the most significant one being $M = 0$ mainly at low $|t|$). A similar result is obtained in the 3π analysis. In fig. 7 we present $d\sigma/dt$ of the A_2 in both decay modes; the agreement is very good. The low statistics of the K^-K^0 data do not allow a precise measurement of polarization as a function of $|t|$. Averaging over the range $0.1 < |t| < 0.3$ GeV^2 where polarization is greater, we get

$$P_N(A_2 \to K^-K^0) = -0.21 \pm 0.12$$
$$P_N(A_2 \to \pi^-\pi^+\pi^-) = -0.25 \pm 0.05 \ .$$

The results are in perfect agreement.

5. RESULTS

5.1 Partial wave intensities

The partial cross-sections for the important J^P_M waves as a function of $m_{3\pi}$ are shown in fig. 8; $J^P_M = 1^+0$ dominates the reaction at low 3π masses. A small but significant contribution of the partial wave 1^+1 $S(\rho\pi)$ is also present. The individual partial waves contributing to the $J^P_M = 1^+0$ enhancement are shown in fig. 9. As found in previous experiments, a single partial wave 1^+0 $S(\rho\pi)$ accounts for 90% of it, the rest being mainly 1^+0 $P(\varepsilon\pi)$. The intensity of the partial wave 1^+0 $D(\rho\pi)$ is negligible.

At higher masses a prominent signal in $J^P_M = 2^+1$ is visible, indicating A_2 production. The superimposed curve in fig. 8 corresponds to a relativistic Breit-Wigner with $M = 1.318$, $\Gamma = 0.110$ GeV. All other waves are minor contributions and show no marked structure.

5.2 Relative phases

In fig. 10 we show the relative phases of the 1^+0 $S(\rho\pi)$ wave with respect to some other partial waves. There are three plots per wave: The first is the phase of the density matrix element as calculated from the amplitudes using

eq. (9). The superimposed lines represent the relative phases obtained in ref. [5]. The other two plots are relative phases of the two transversity amplitudes $S = \pm 1/2$. In the density matrix phases with respect to 0^-0 $S(\varepsilon\pi)$ and 1^+0 $P(\varepsilon\pi)$, little or no variation is seen. However, an increase of about 60-90 degrees is observed in the relative phases of 2^-0 $P(\rho\pi)$ and 2^+1 $D(\rho\pi)$ [in the latter we have subtracted the Breit-Wigner phase of the A_2 in order to see variations due to 1^+0 $S(\rho\pi)$]. Our results are in perfect agreement with the results from ref. [5]. Qualitatively the same behaviour is observed in the two transversity amplitude phases. This fact provides a good check of the validity of the coherence assumption. In this case, to identify the density matrix phase with the amplitude phase is therefore a good approximation.

Variations in the relative phase with respect to the 0^-0 $P(\rho\pi)$ partial wave were also observed in ref. [5]. In our case this partial wave is very strongly affected by ambiguities, and the relative phase (not shown) is not well determined.

Since the relative phases we determined agree very well with those from ref. [5], an interpretation of our results in terms of direct A_1 production interfering with a unitarized Deck-type background would lead to very similar conclusions. In particular, the A_1 must be rather wide with a mass in the range 1.2-1.3 GeV. The lack of phase variation with respect to the 0^-0 $S(\varepsilon\pi)$ wave remains a problem. A possible 0^- resonance is by no means excluded. This situation is very similar to the one found in the $K\pi\pi$ analysis of Brandenburg et al. [18], where it is claimed that the Q_2 is also accompanied by a 0^- (εK) resonance. The constant phase relative to 1^+0 $P(\varepsilon\pi)$ could be understood if the resonance couples to $\varepsilon\pi$ as well as to $\rho\pi$.

5.3 Nucleon polarization

The total nucleon polarization P_N obtained using the right-left asymmetry of section 2.3 can be compared with the one obtained from the amplitudes in the partial wave analysis. They are in very good agreement, indicating that acceptance corrections for this quantity are very small. The P_N is shown as a function of $m_{3\pi}$ in fig. 11a; it is negative in the whole mass range except in the region 1.15-1.2 GeV, where it is compatible with 0.

The t-dependence of P_N is shown in fig. 11b. It looks very similar to $\pi^- p$ elastic scattering. The superimposed curves are the predictions from a Deck model [19]. Apart from the possible structure around 1.2 GeV, the agreement is reasonable. One should note that several models could lead to P_N similar to elastic scattering. Semi-inclusive duality [1] predicts an increase of P_N with $m_{3\pi}$, which seems not to be the case.

The nucleon polarization of individual partial waves as defined in eq. (12) suffers from ambiguities and also from large fluctuations in most of the minor waves. In fig. 12 we show the polarization for the major contribution $J^P_M = 1^+0$ as a function of $m_{3\pi}$. It is negative and exhibits a pattern very similar to the total 3π polarization. In particular, the structure around 1.2 GeV is still present. Such behaviour could be understood in terms of the rescattering models mentioned in the introduction [7,8]. The deviation from a Breit-Wigner shape is obtained in these models by an additional zero in the amplitude as a function of $m_{3\pi}$. The position of this zero depends on the relative amount of direct production and unitarized Deck-type background. If the position of the zero is different for spin-non-flip and spin-flip amplitudes (especially the zero in the spin-flip must occur below the resonance), the polarization will exhibit a zero. It is interesting to mention that relative phases will not be affected since both amplitudes have the same A_1 resonance phase, and the same applies to intensities since spin-non-flip will dominate. The presence of non-resonant background could also shift the position of the zero in the polarization. This, together with the poor statistical significance of the effect, prevents us making a detailed fit. We can only state that, qualitatively, the observed polarization is not in disagreement with the A_1 production mechanism obtained in ref. [5].

The 2^+1 polarization is only well defined in the A_2 region. In the range $1.2 < m_{3\pi} < 1.4$ GeV we get an average polarization of

$$P_N(A_2) = -0.25 \pm 0.05 \ ,$$

in good agreement with that obtained in the K^0K^- decay mode as mentioned in section 4.

6. CONCLUSIONS

The reaction $\pi^- p_\uparrow \to \pi^-\pi^+\pi^- p$ at 17 GeV/c has been measured and a partial wave analysis of the 3π system performed using the isobar model. The acceptance correction for the nucleon polarization turns out to be negligible. This nucleon polarization is negative and roughly independent of 3π mass, except for a possible structure around 1.2 GeV which appears also in the 1^+0 wave partial polarization. As a function of t, the nucleon polarization is similar to $\pi^- p$ elastic scattering as predicted by the Deck model. The nucleon polarization for A_2 production is also negative. By averaging in the region $1.2 < m_{3\pi} < 1.4$ GeV we obtained $P_N(A_2) = -0.25 \pm 0.05$ in the t interval $0.1 < |t| < 0.3$ GeV^2.

Detailed information about resonance production has recently been obtained in an experiment using an unpolarized hydrogen target. We have checked the coherence assumption made in their analysis [5], by comparing the relative phases between our transversity amplitudes with the density matrix ones. All three phases agree well and are also compatible with the ones from ref. [5]. Therefore our results support their conclusions concerning the A_1 resonance. The lack of phase variation of the 1^+0 $S(\rho\pi)$ wave with respect to the 0^-0 $S(\varepsilon\pi)$ wave suggests, as a possible explanation, the existence of a 0^- resonance.

Acknowledgements

We are grateful to G. Ascoli and R. Klanner for many helpful discussions.

APPENDIX 1

In this Appendix we discuss our determination of the fraction of events from polarized protons. The $\Delta\Phi$ distribution shown in fig. 2 consists of many components, including one from polarized free protons. Our method was to fit the $\Delta\Phi$ distribution using our best estimate of these components.

During the experiment we accumulated a sample of π^-p elastic events. We fitted the $\Delta\Phi$ distribution of these elastic events in three different $|t|$ bins (0.1-0.2, 0.2-0.4, 0.4-1.0 GeV) with a shape of the form

$$\frac{dN}{d(\Delta\Phi)} = N_H f_H(\Delta\Phi) + N_Q f_Q(\Delta\Phi) + N_I f_I(\Delta\Phi) + N_F f_F(\Delta\Phi) = \sum_i N_i f_i(\Delta\Phi) \ ;$$

i) H is the free proton contribution, the shape $f_H(\Delta\Phi)$ being determined from events produced on a liquid-hydrogen target.

ii) Q is the quasi-elastic contribution from bound protons. The shape for $f_Q(\Delta\Phi)$ was calculated using an harmonic oscillator version of the shell model with P-wave and S-wave momentum-space wave functions. The harmonic oscillator parameters were taken from the measurements of ref. [20].

iii) I is a genuine inelastic contribution due to events such as $\pi^-p \to \pi^-\pi^0p$, for which the shape was determined using events with high missing mass.

iv) F is a flat background to account for other sources besides (i), (ii), and (iii).

After some adjustments of the function f_i, we succeeded in producing good fits on π^-p elastic data. We then used the same functions to fit the 3π data, using the same $|t|$ bins with the normalization constants N_i as the only free parameters.

The results of these fits on butanol data gave, for a 5° cut in $|\Delta\Phi|$, free proton fractions of 0.8 ± 0.05, 0.66 ± 0.05, and 0.46 ± 0.05, respectively. The same cut on π^-p elastic butanol data gave fractions of 0.84, 0.72, and 0.60 in these $|t|$ bins. As a check, the same procedure was applied to the 3π reaction from the hydrogen data sample. We obtained fractions of 0.99 ± 0.01, 0.98 ± 0.02, and 0.92 ± 0.03 in the same $|t|$ bins, the $\Delta\Phi$ cut of ±5° being 80% efficient. In

the range 0.1-0.3 GeV, where most of our attention is concentrated, this latter check gives us confidence in our procedure.

APPENDIX 2

Following the method described in ref. [11], the B matrix of expressions (5) and (8) can be obtained; it is as follows:

	$\eta = +1$ $S = +1/2$	$\eta = +1$ $S = -1/2$	$\eta = -1$ $S = +1/2$	$\eta = -1$ $S = -1/2$
$\eta = +1$ $S = +1/2$	$1 + \alpha \cos \psi$	0	$- i \alpha \sin \psi$	0
$\eta = +1$ $S = -1/2$	0	$1 - \alpha \cos \psi$	0	$+ i \alpha \sin \psi$
$\eta = -1$ $S = +1/2$	$+ i \alpha \sin \psi$	0	$1 - \alpha \cos \psi$	0
$\eta = -1$ $S = -1/2$	0	$- i \alpha \sin \psi$	0	$1 + \alpha \cos \psi$

ψ is described in the text (see section 3). The α factor is a product of two terms: the first one, α_1, is the average target polarization ($\alpha_1 = 0.68$); the second one, α_2, is the fraction of interactions on free protons obtained, as described in Appendix 1.

REFERENCES

[1] G. Hoehler et al., Nucl. Phys. B114 (1976) 505.

[2] P. Gavillet et al., Phys. Lett. 69B (1977) 119.

A. Ferrer et al., Nucl. Phys. B142 (1978) 77.

[3] G. Alexander et al., DESY 77/78 (1978).

[4] F. Wagner et al., Phys. Lett. 58B (1975) 201.

C. Baltay et al., Phys. Rev. Lett. 39 (1977) 591.

M.J. Emms et al., Phys. Lett. 58B (1975) 117.

M. Cerrada et al., Nucl. Phys. B126 (1977) 241.

[5] C. Daum et al., Phys. Lett. 89B (1980) 281.

[6] For a review of 3π experiments earlier than ref. [5] see, for example, M. Cerrada, Proc. 6th Int. Winter Meeting on Fundamental Physics, El Paular (Spain), 1978.

[7] M.G. Bowler et al., Nucl. Phys. B97 (1975) 227.

[8] J.L. Basdevant and E. Berger, Phys. Rev. D 16 (1977) 657.

[9] H. De Groot, Ph.D. thesis, Amsterdam, 1978.

[10] H. Becker et al., Nucl. Phys. B150 (1979) 301.

H. Becker et al., Nucl. Phys. B151 (1979) 46.

[11] F. Wagner, Nucl. Phys. B111 (1976) 67.

[12] J.D. Hansen et al., Nucl. Phys. B81 (1974) 403.

[13] D.V. Brockway, Ph.D. thesis, Univ. Illinois, Report No. COO-1195-197 (1970); and also ref. [12].

[14] B. Hyams et al., Nucl. Phys. B63 (1973) 153.

[15] J. Orear, UCRL-8417 (1958).

[16] G. Ascoli et al., Phys. Rev. Lett. 25 (1970) 962.

[17] V. Chabaud et al., preprint CERN-EP/79-159 (1979).

[18] G.W. Brandenburg et al., Phys. Rev. Lett. 36 (1976).

[19] J. Wildeneuer, Diplom Arbeit Universität München (1980).

J. Wildeneuer and F. Wagner, to be published.

[20] A.N. James et al., Nucl. Phys. A133 (1969) 89.

Table 1

Partial waves included
in the present analysis

	ℓ	Decay mode
0^-0	S	$\varepsilon\pi$
	P	$\rho\pi$
1^+0	S	$\rho\pi$
	P	$\varepsilon\pi$
	D	$\rho\pi$
1^+1	S	$\rho\pi$
	P	$\varepsilon\pi$
2^-0	S	$\rho\pi$
	P	$\rho\pi$
	D	$\varepsilon\pi$
2^+1	D	$\rho\pi$

Figure captions

Fig. 1 : Schematic top view of the CERN-Munich spectrometer. The lower part shows a front view of the target region with the disposition of the F counters and target hodoscope.

Fig. 2 : Distribution of the coplanarity angle $\Delta\Phi$; $\Delta\Phi$ is the angle between the recoil proton direction obtained from the 3π and incident beam measured momenta and the direction obtained from the target hodoscope information

a) in 4° bins for a subsample containing about 15% of the data;

b) in 1° bins for the whole sample in the range $|\Delta\Phi| < 20°$.

Fig. 3 : Missing-mass squared distribution for coplanar events ($|\Delta\Phi| < 5°$).

Fig. 4 : a) $|t|$ distribution for coplanar events having missing-mass squared < 1.35 GeV;

b) $m_{3\pi}$ distribution for events with the same cuts as in fig. 4a and $|t| > 0.1$ GeV^2.

Fig. 5 : Sample of events used in the partial wave analysis (see text).

a) $\pi^+\pi^-$ mass distribution (two entries per event);

b) $\pi^-\pi^-$ mass distribution.

Fig. 6 : $A(\phi)$ distribution. $A(\phi)$ is defined in the following way:

$$A(\phi) = \frac{N_{up}(\phi) - N_{down}(\phi)}{N_{up}(\phi) + N_{down}(\phi)} ,$$

ϕ being the azimuthal angle. The superimposed curve corresponds to the result of a fit with a parametrization $\alpha \sin \phi$.

Fig. 7 : $dN/d|t|$ for A_2 production as a function of $|t|$. The solid circles correspond to the 3π decay mode and the open ones to the K^-K^0 decay mode. The superimposed curves correspond to a parametrization of the form $t \cdot e^{Bt}$, with $B = -7.5$ GeV^{-2}.

Fig. 8 : Cross-section $dN/dm_{3\pi}$ for the important J^PM states summed over various decay channels as a function of 3π mass. The expected Breit-Wigner shape from the A_2 resonance is superimposed on the 2^+1 intensity.

Fig. 9 : Cross-section $dN/dm_{3\pi}$ for the partial waves contributing to $J^PM = 1^+0$ [1^+0 S($\rho\pi$), 1^+0 P($\varepsilon\pi$), 1^+0 S($\rho\pi$)] as a function of 3π mass.

Fig. 10 : Relative phase between the 1^+0 S($\rho\pi$) partial wave and several reference waves as a function of 3π mass. The plots in the first column correspond to density matrix phases, and the superimposed lines indicate the results from ref. [8]. The second and third column plots are phases between the $S = \frac{1}{2}$ and $S = -\frac{1}{2}$ amplitudes, respectively. In the 2^+1 D($\rho\pi$) wave, a Breit-Wigner A_2 phase has been subtracted.

Fig. 11 : Nucleon polarization P_N:
a) as a function of $m_{3\pi}$ in the $|t|$ interval $0.1 < |t| < 0.3$ GeV^2;
b) as a function of $|t|$ in the $m_{3\pi}$ interval $1.0 < m_{3\pi} < 1.4$ GeV.
The superimposed curves are predictions from a Deck model.

Fig. 12 : Nucleon polarization P_N for the $J^PM = 1^+0$ waves alone as a function of $m_{3\pi}$. The solid curve gives the Deck model prediction for the dominant 1^+0 S($\rho\pi$) contribution.

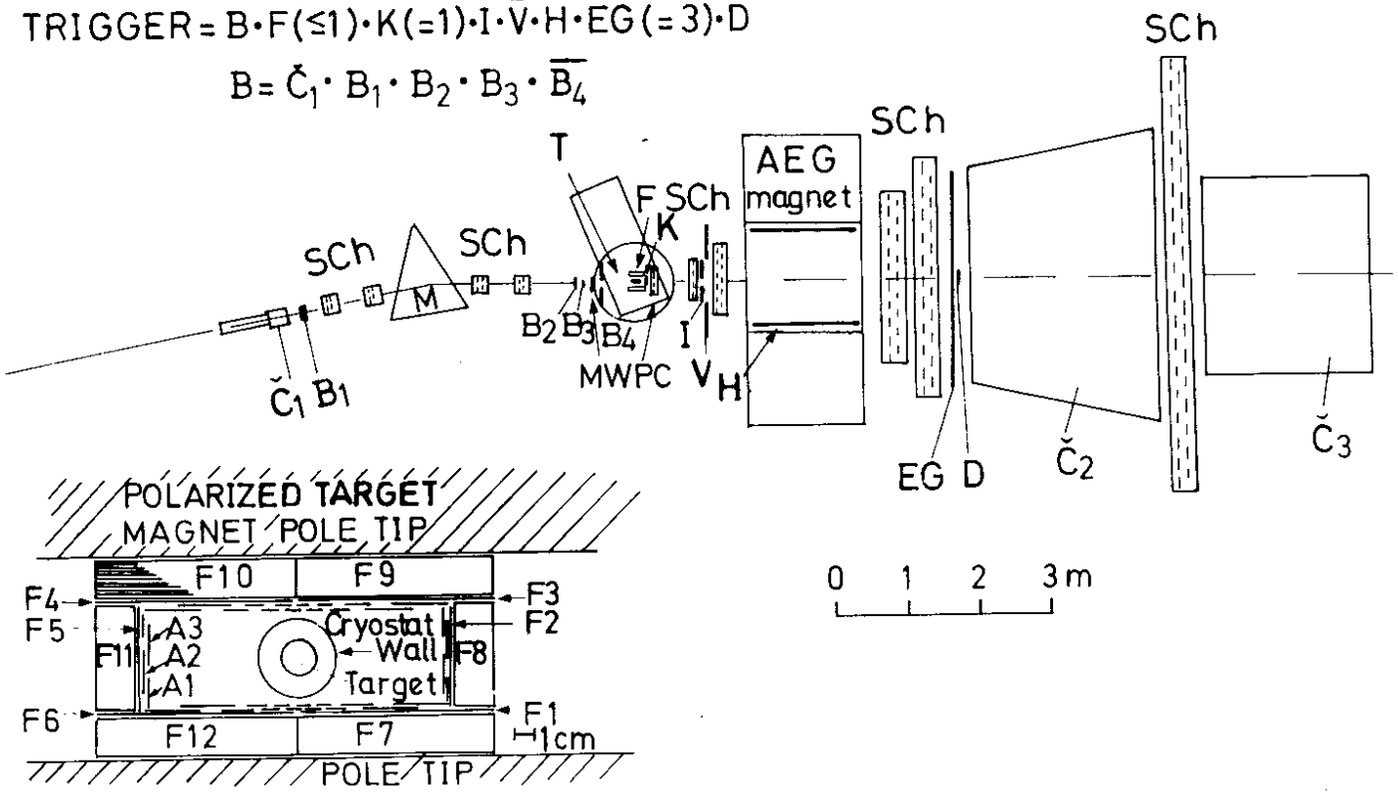
TRIGGER = B·F(≤1)·K(=1)·I·V̄·H̄·EG(=3)·D̄
B = Č1 · B1 · B2 · B3 · B̄4
SCh
SCh
SCh
T
F
K
SCh
AEG
magnet
M
B2
B3
B4
MWPC
I
V
H
Č1
B1
EG
D
Č2
Č3
0 1 2 3m
POLARIZED TARGET
MAGNET POLE TIP
F10
F9
F4
F5
F3
F2
F11
A3
A2
A1
Cryostat
Wall
Target
F8
F6
F12
F7
F1
1cm
POLE TIP

Fig. 1

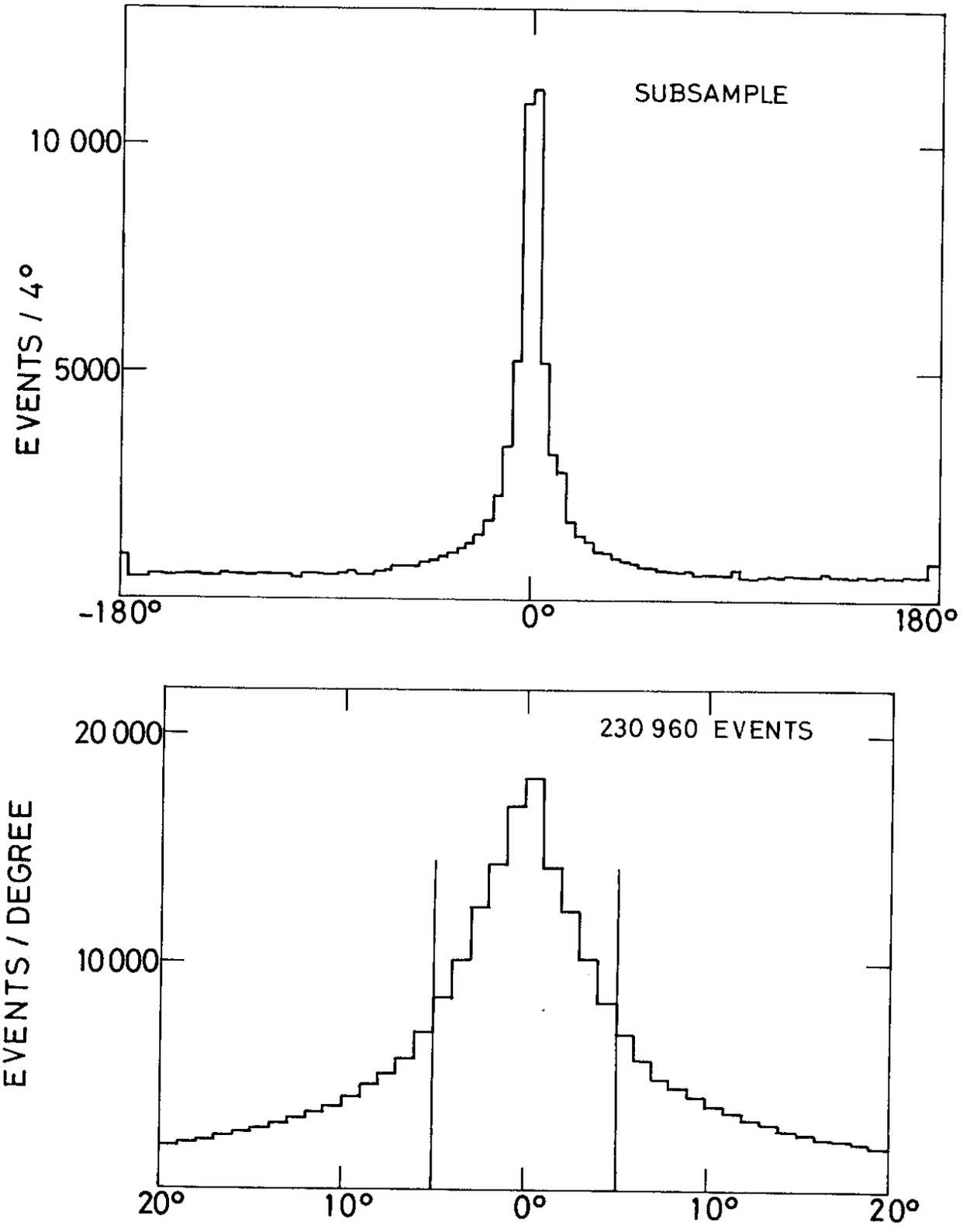
SUBSAMPLE
10 000
5000
EVENTS / 4°
-180°
0°
180°
230 960 EVENTS
20 000
10000
EVENTS / DEGREE
20°
10°
0°
10°
20°

Fig. 2

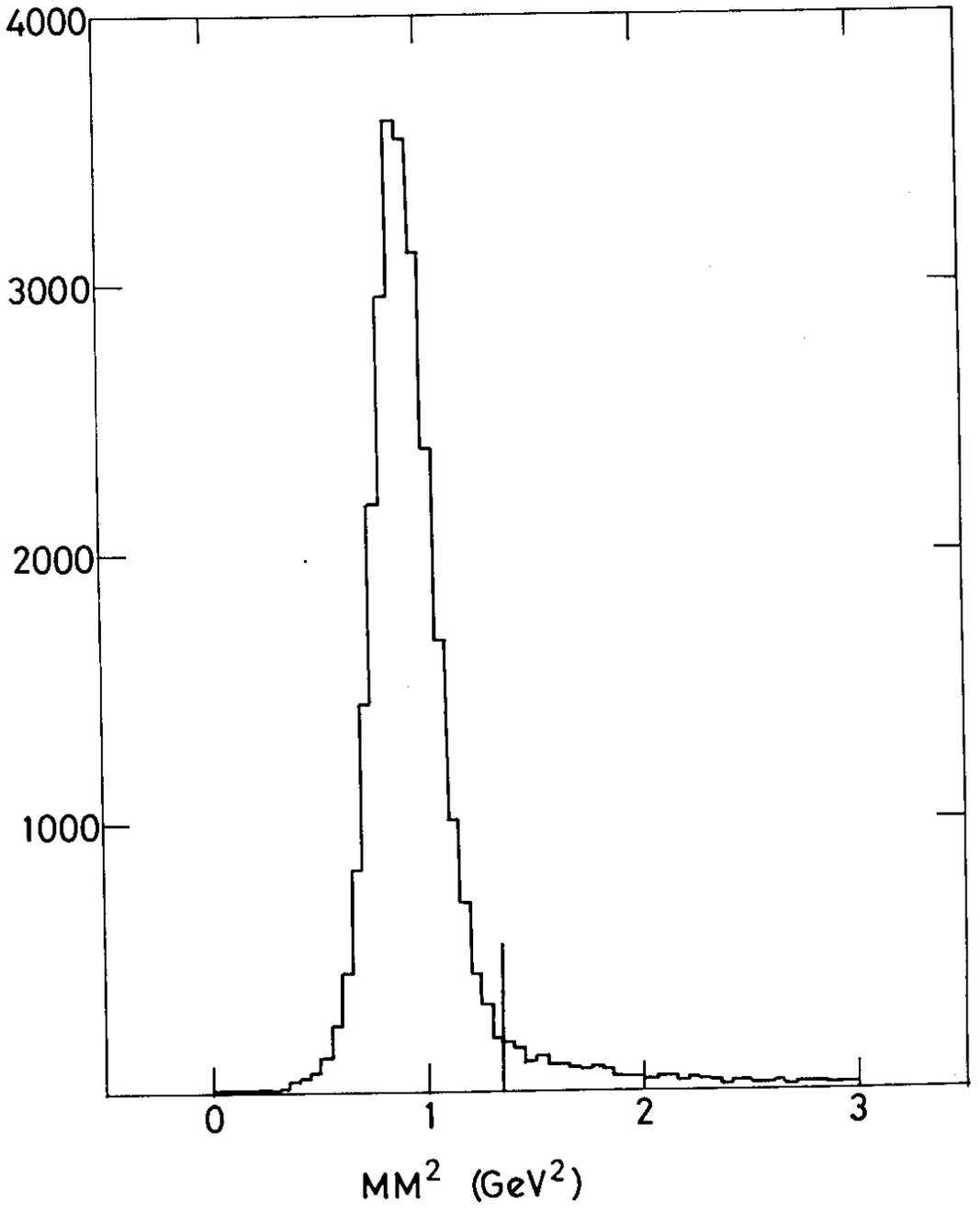

Fig. 3

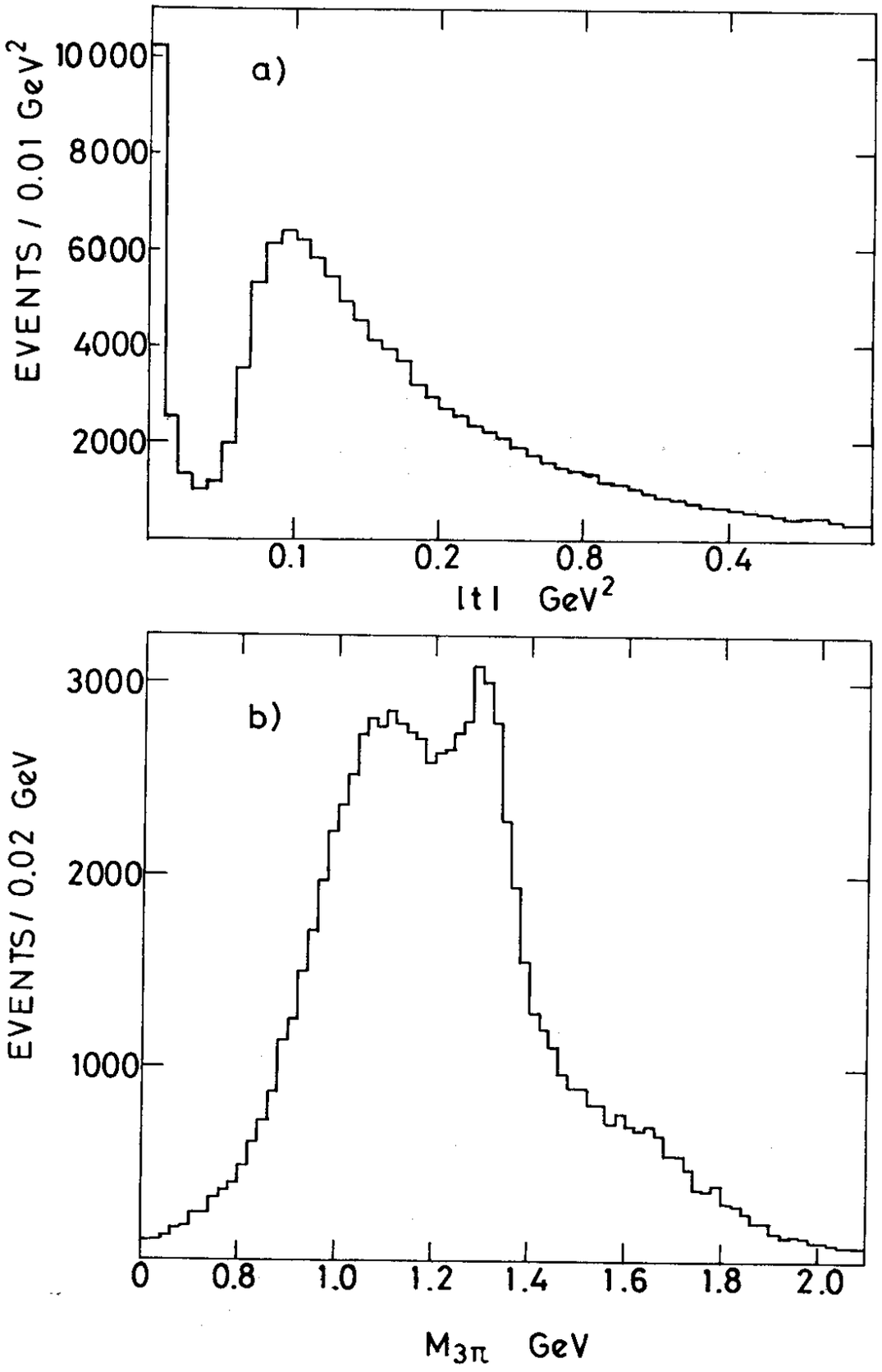
a)
EVENTS / 0.01 GeV²
10000
8000
6000
4000
2000
0.1
0.2
0.8
0.4
|t| GeV²
b)
EVENTS / 0.02 GeV
3000
2000
1000
0
0.8
1.0
1.2
1.4
1.6
1.8
2.0
M3π GeV

Fig. 4

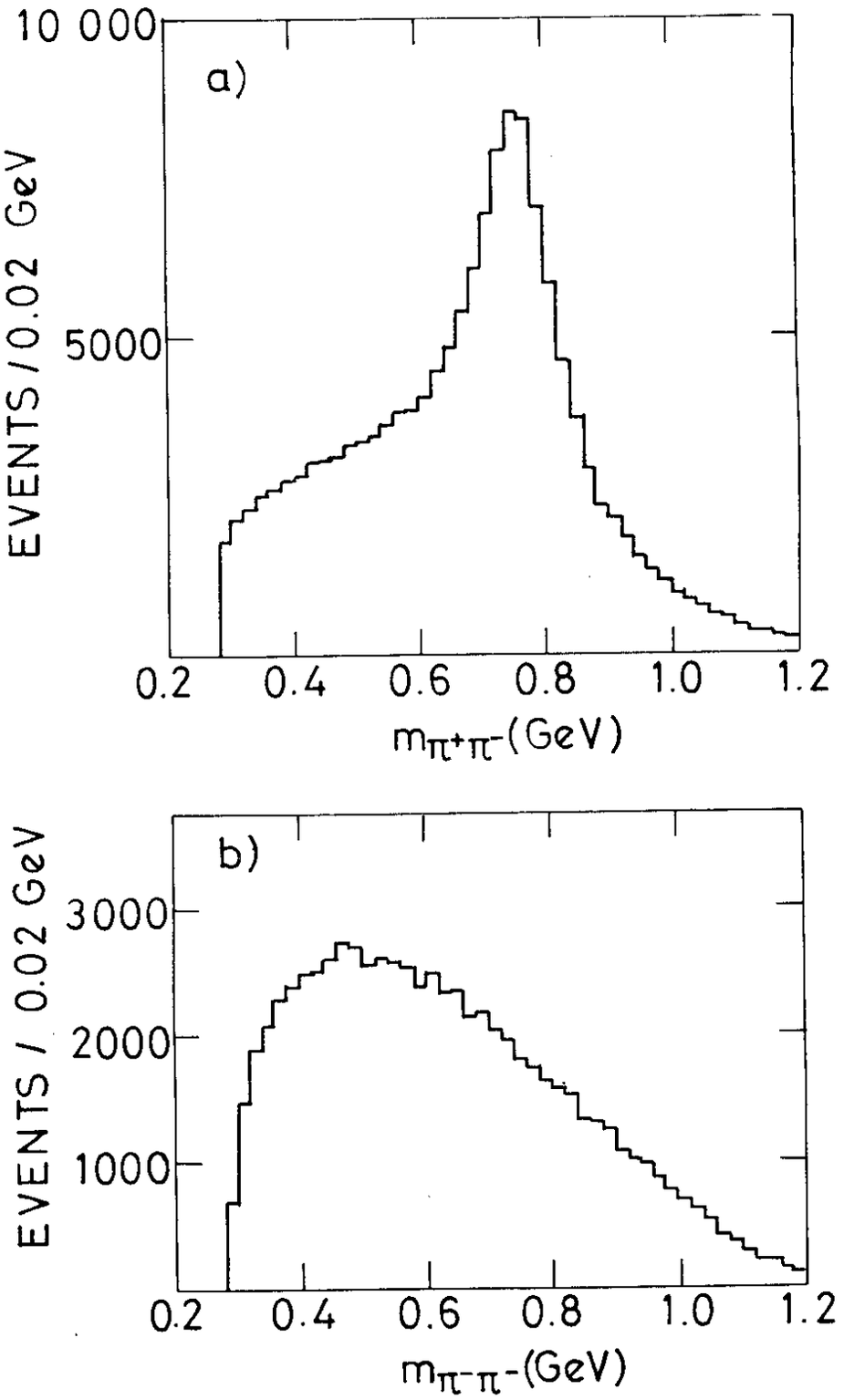
a)
10 000
5000
EVENTS / 0.02 GeV
0.2
0.4
0.6
0.8
1.0
1.2
$m_{\pi^+\pi^-}$(GeV)
b)
3000
2000
1000
EVENTS / 0.02 GeV
0.2
0.4
0.6
0.8
1.0
1.2
$m_{\pi^-\pi^-}$(GeV)

Fig. 5

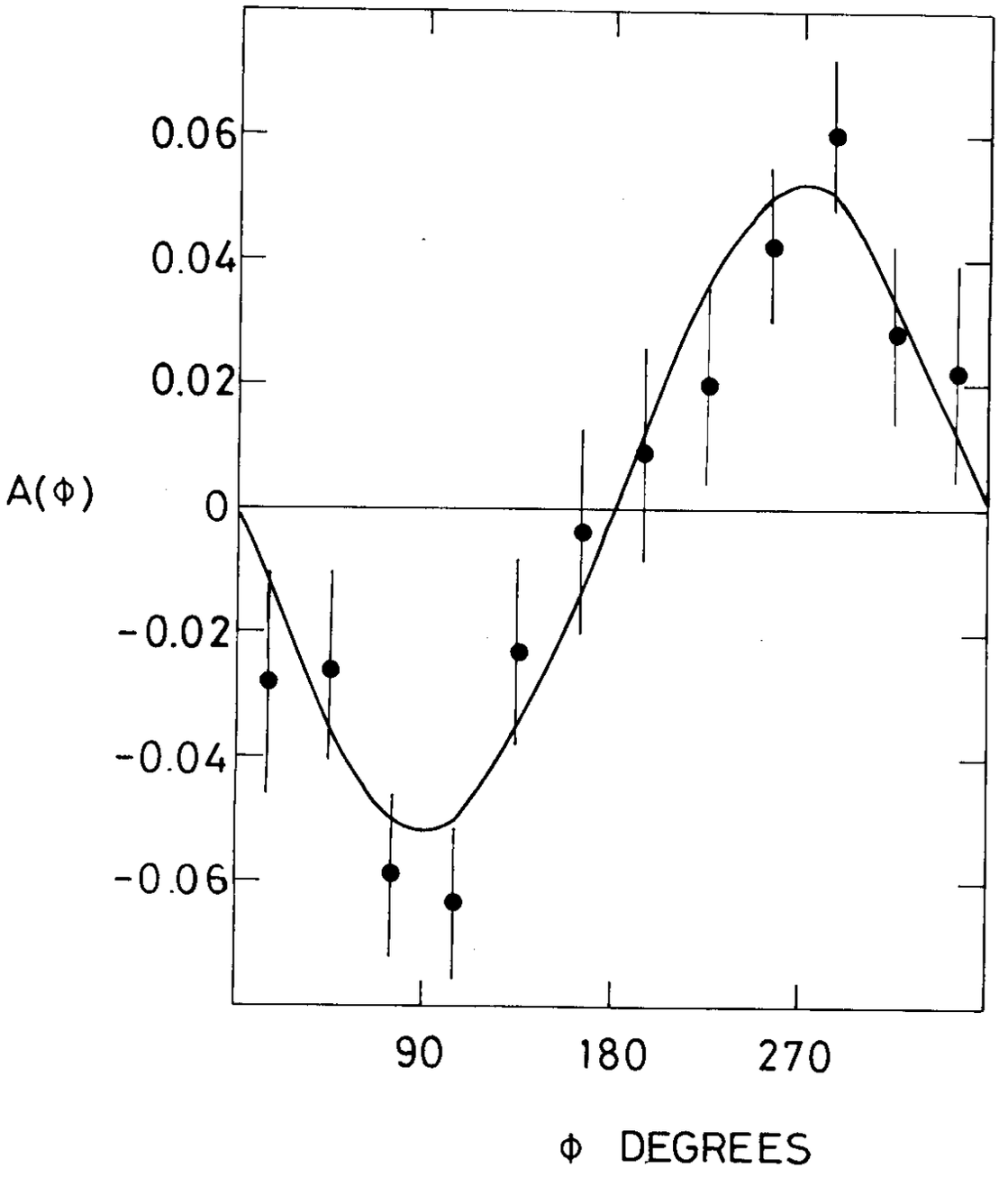

Fig. 6

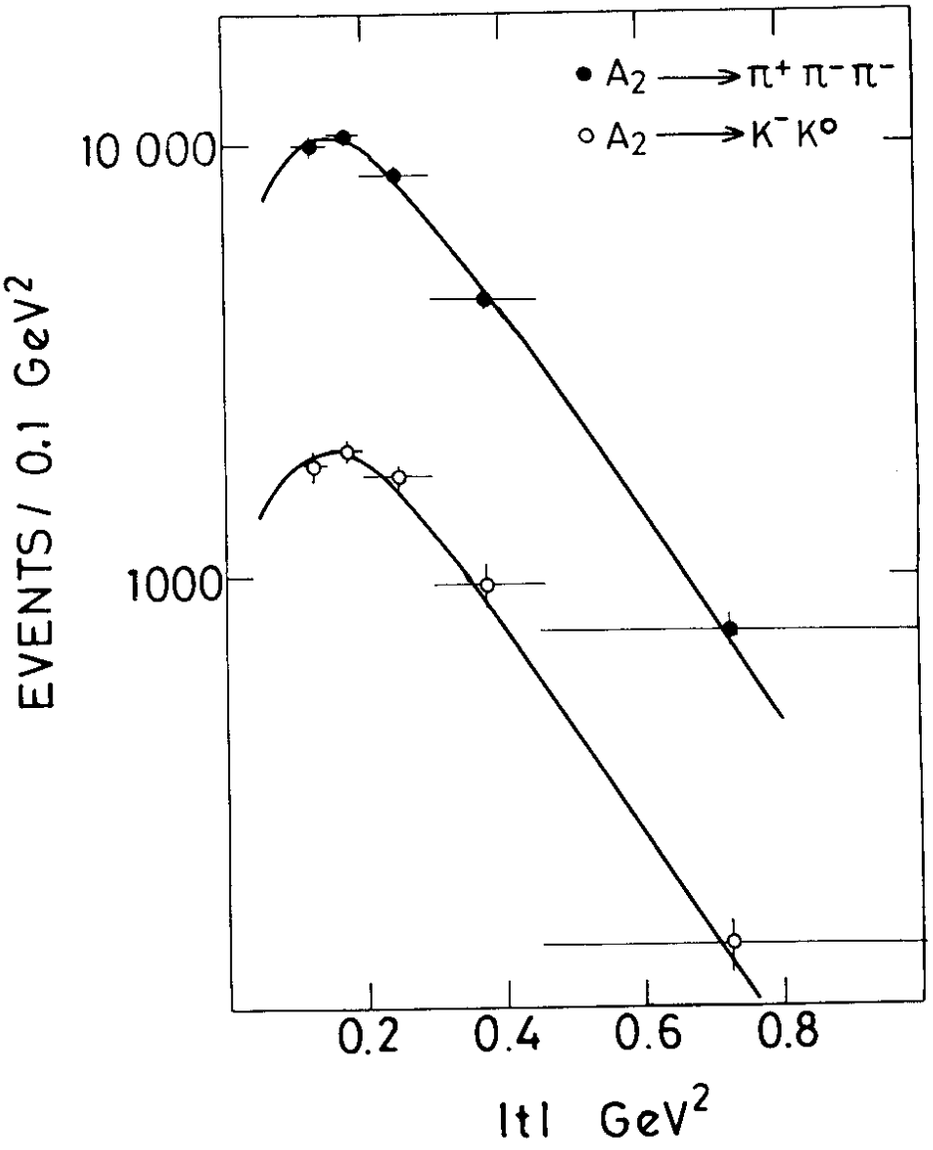
• $A_2 \longrightarrow \pi^+ \pi^- \pi^-$
○ $A_2 \longrightarrow K^- K^0$
10 000
1000
EVENTS / 0.1 GeV²
0.2
0.4
0.6
0.8
|t| GeV²

Fig. 7

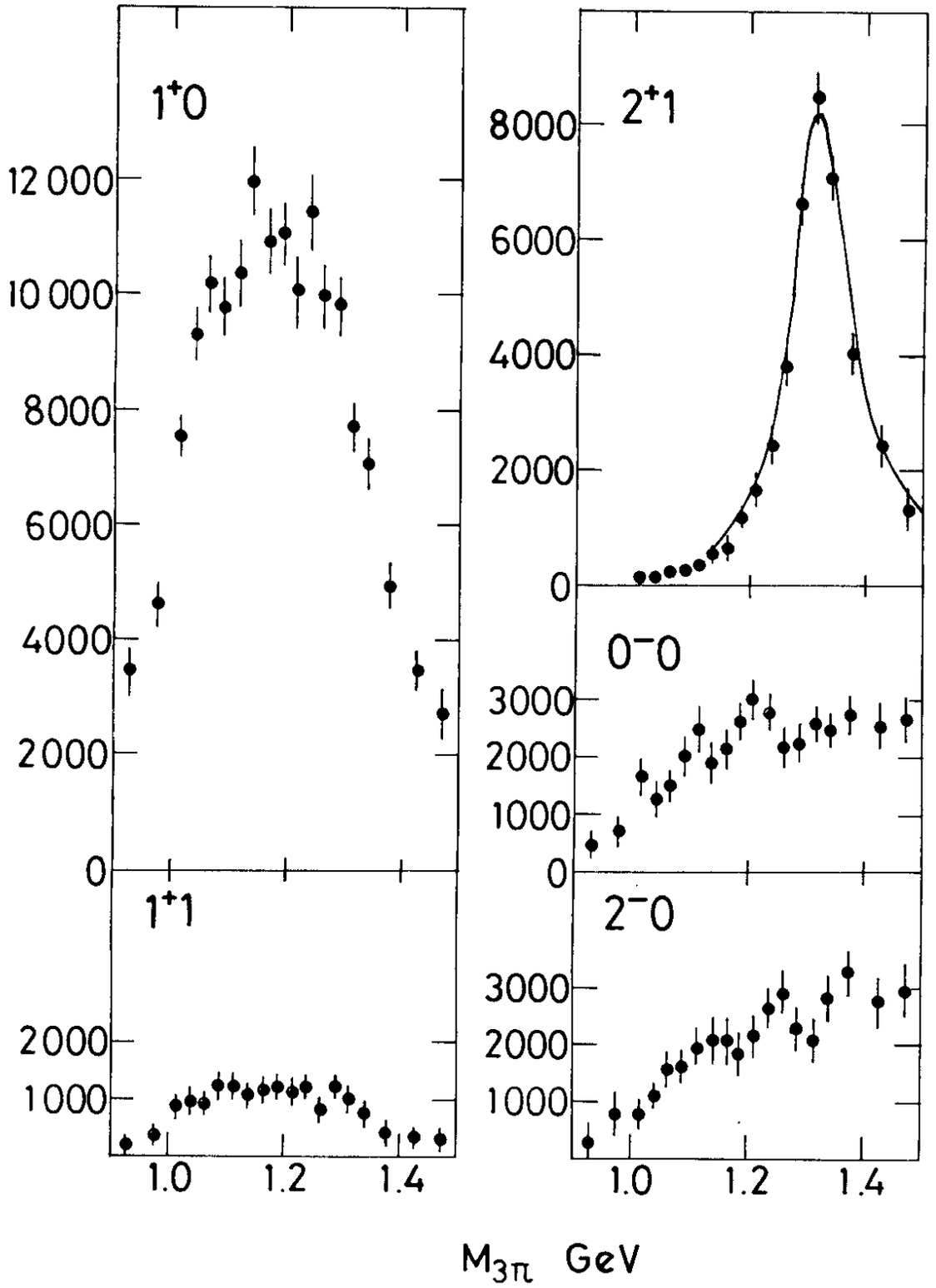
1⁺0
12 000
10 000
8000
6000
4000
2000
0
1⁺1
2000
1000
2⁺1
8000
6000
4000
2000
0
0⁻0
3000
2000
1000
0
2⁻0
3000
2000
1000
1.0
1.2
1.4
M3π GeV

Fig. 8

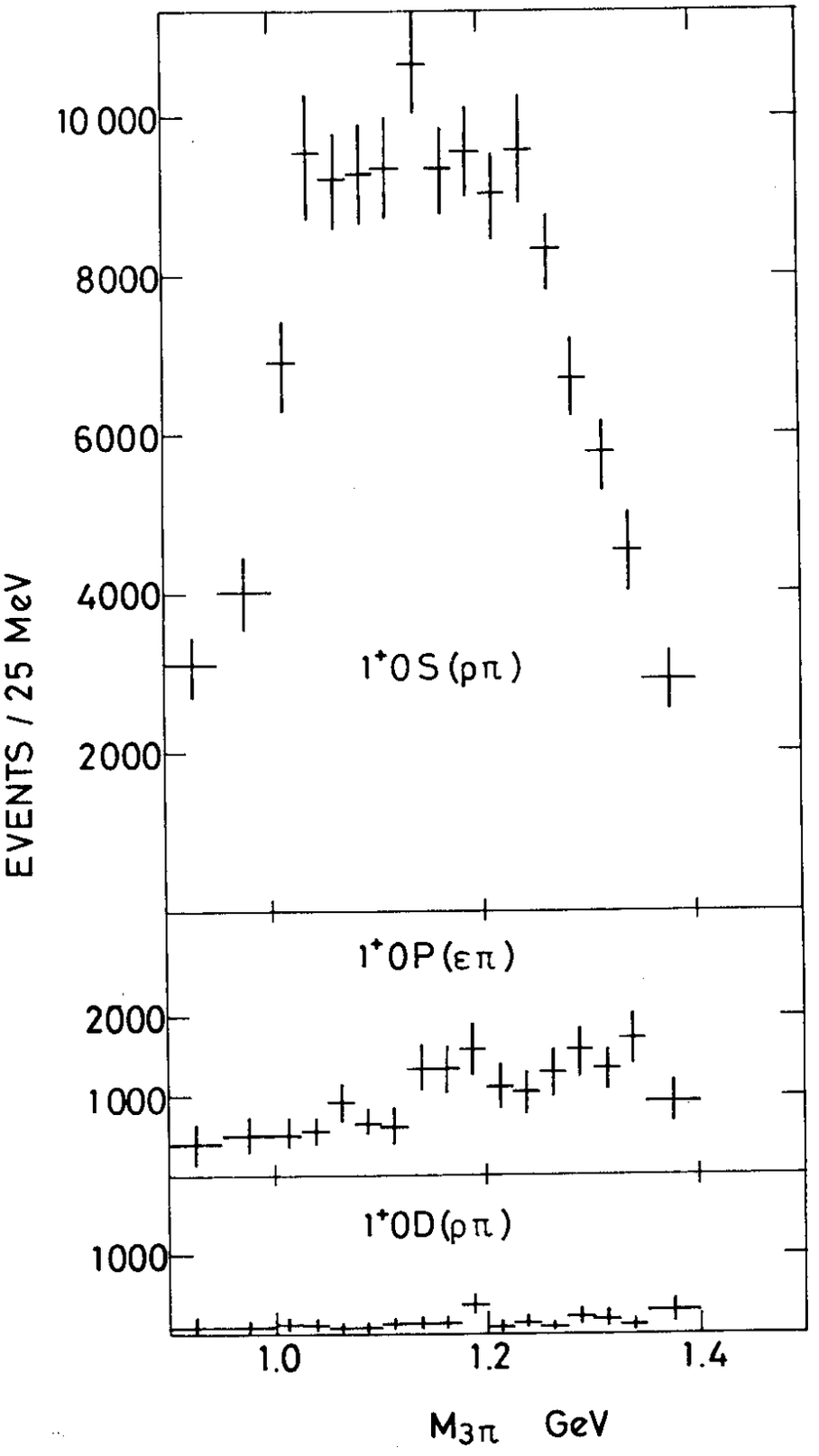
10 000
8000
6000
4000
2000
EVENTS / 25 MeV
1⁺0S(ρπ)
1⁺0P(επ)
2000
1000
1⁺0D(ρπ)
1000
1.0
1.2
1.4
M3π GeV

Fig. 9

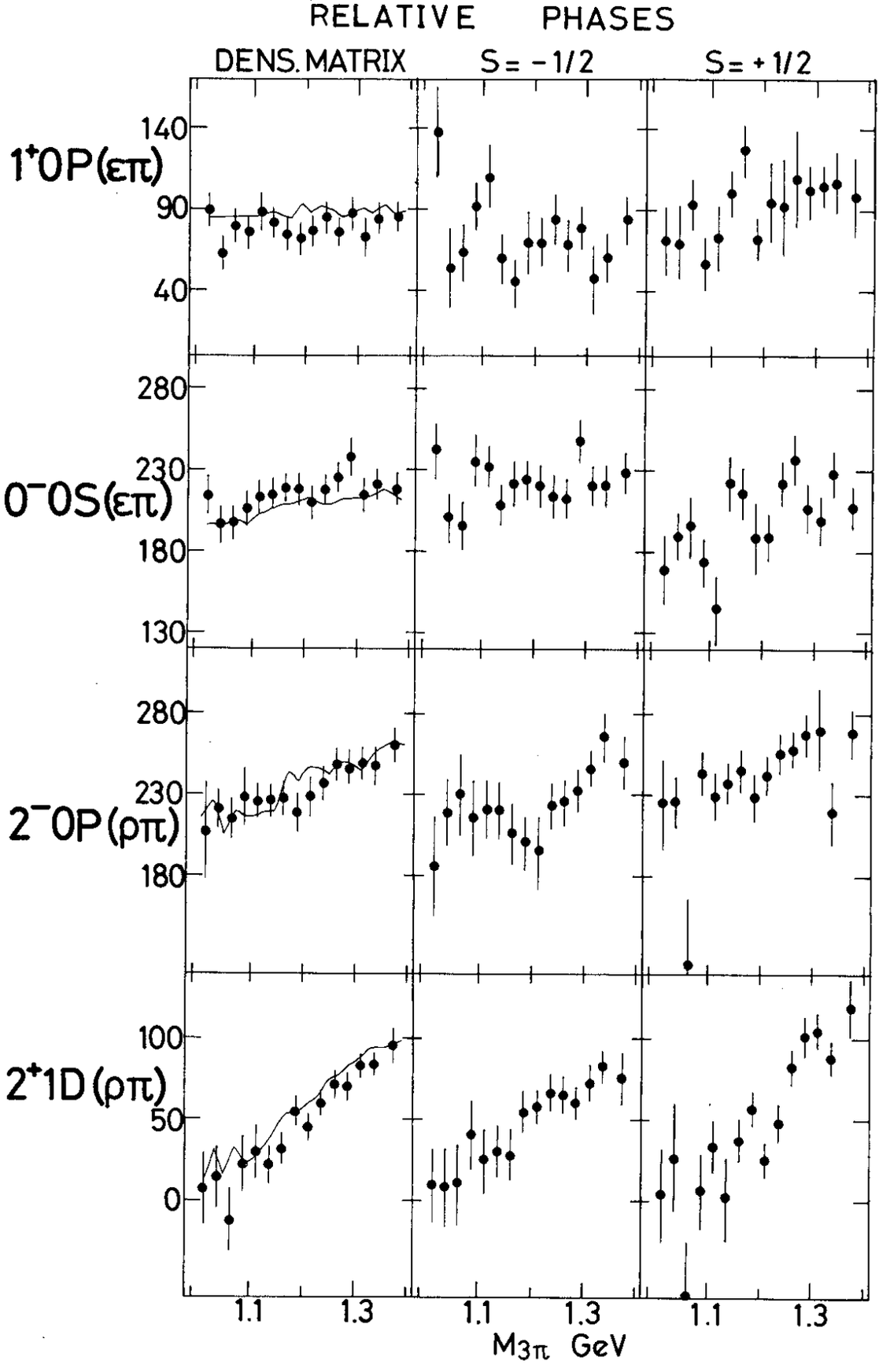
RELATIVE PHASES
DENS. MATRIX
S = -1/2
S = +1/2
1+0P(επ)
0-0S(επ)
2-0P(ρπ)
2+1D(ρπ)
140
90
40
280
230
180
130
280
230
180
100
50
0
1.1
1.3
1.1
1.3
1.1
1.3
M3π GeV

Fig. 10

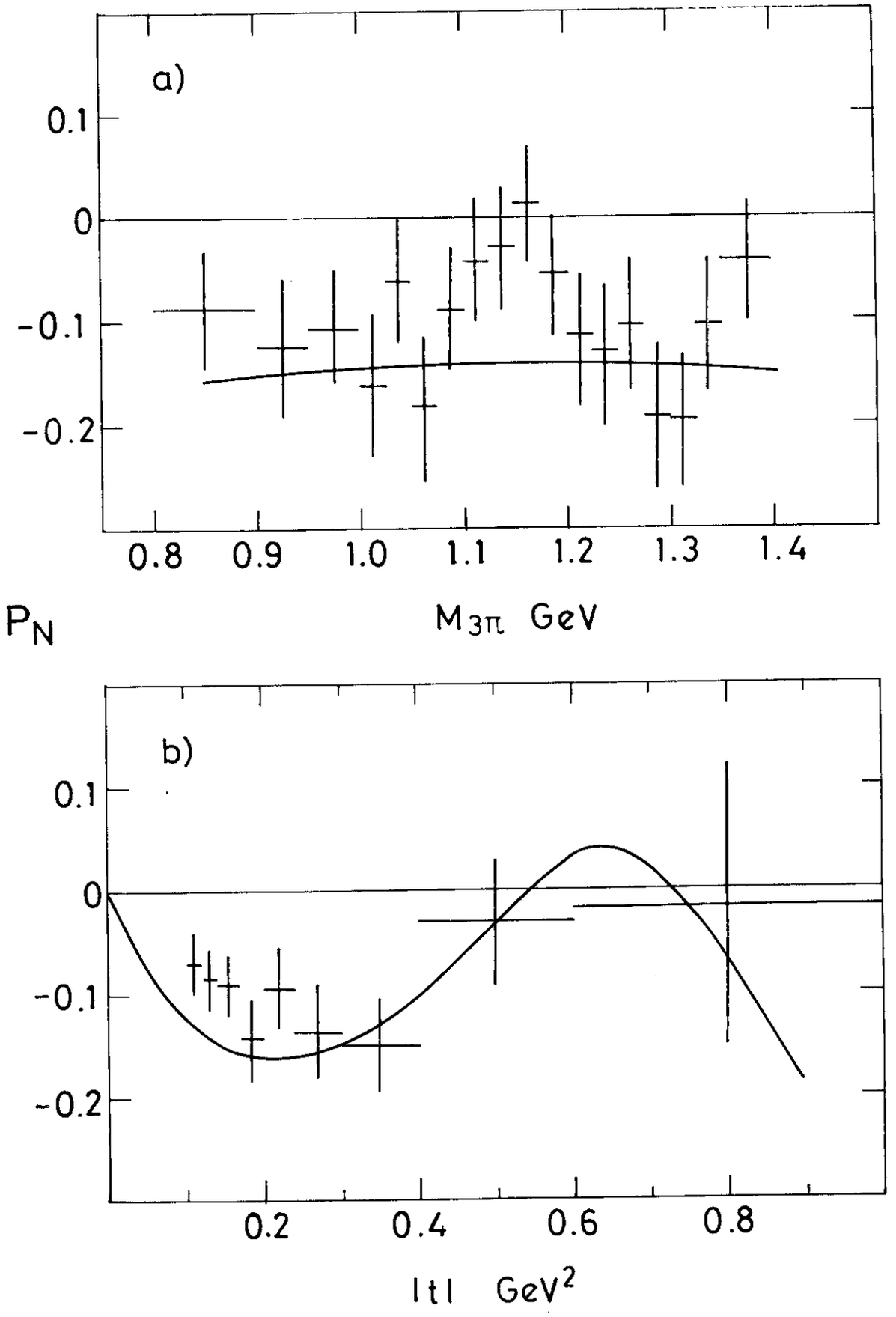
a)
0.1
0
-0.1
-0.2
0.8
0.9
1.0
1.1
1.2
1.3
1.4
P_N
$M_{3\pi}$ GeV
b)
0.1
0
-0.1
-0.2
0.2
0.4
0.6
0.8
$|t|$ GeV^2

Fig. 11

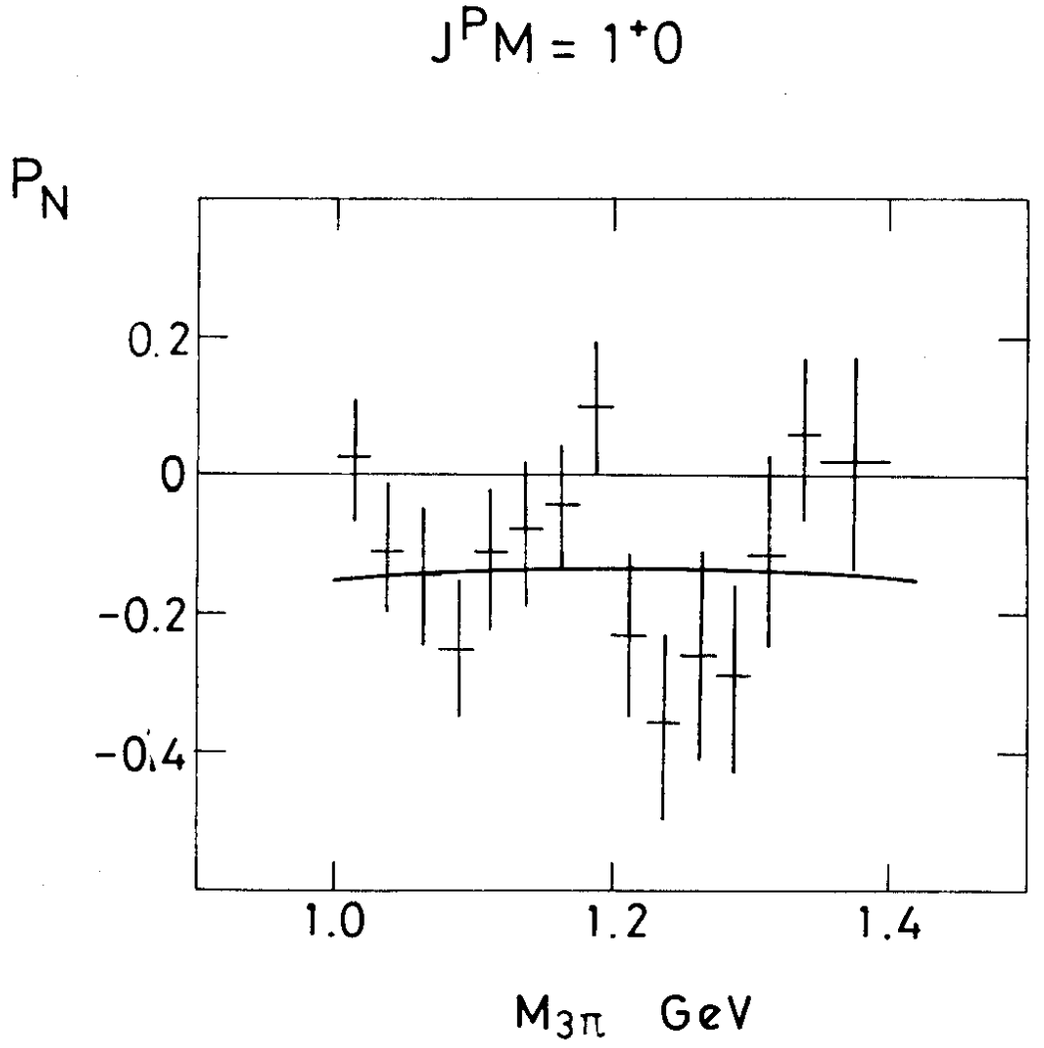

Fig. 12